Improved charge-trapping properties of HfYON film for nonvolatile memory applications in comparison with HfON and Y2O3 films

X. D. Huang, L. Liu, J. P. Xu, and P. T. Lai

Citation: Applied Physics Letters **99**, 112903 (2011); doi: 10.1063/1.3639275
View online: http://dx.doi.org/10.1063/1.3639275
View Table of Contents: http://scitation.aip.org/content/aip/journal/apl/99/11?ver=pdfcov
Published by the AIP Publishing

Improved charge-trapping properties of HfYON film for nonvolatile memory applications in comparison with HfON and Y_2O_3 films

X. D. Huang,[1] L. Liu,[2] J. P. Xu,[2] and P. T. Lai[1,a)]
[1]*Department of Electrical & Electronic Engineering, The University of Hong Kong, Pokfulam Road, Hong Kong*
[2]*Department of Electronic Science & Technology, Huazhong University of Science and Technology, Wuhan 430074, People's Republic of China*

(Received 9 June 2011; accepted 12 August 2011; published online 14 September 2011)

The charge-trapping properties of HfYON film are investigated by using the Al/HfYON/SiO_2/Si structure. The physical features of this film were explored by transmission electron microscopy and x-ray photoelectron spectroscopy. The proposed device shows better charge-trapping characteristics than samples with HfON or Y_2O_3 as the charge-trapping layer due to its higher trapping efficiency, as confirmed by extracting their charge-trap centroid and charge-trap density. Moreover, the Al/Al_2O_3/HfYON/SiO_2/Si structure shows high program speed (4.5 V at +14 V, 1 ms), large memory window (6.0 V at ±14 V, 1 s), and good retention property, further demonstrating that HfYON is a promising candidate as the charge-trapping layer for nonvolatile memory applications. © *2011 American Institute of Physics*. [doi:10.1063/1.3639275]

Charge-trapping nonvolatile (CTN) memories with dielectrics as charge storage layers have attracted increasing interest due to their lower power consumption, higher reliability, and easier dimension scaling than their floating-gate counterparts. Recently, different high-*k* dielectrics have been proposed as charge-trapping layer (CTL) instead of Si_3N_4, mainly due to their high charge-trapping efficiency and high scaling ability.[1–6] A charge-trap-engineered (CTE) memory with dual trapping layers was also proposed to obtain high program/erase (P/E) speeds and good retention property, and a high-*k* dielectric with high deep-level charge-trap density was also desirable for this CTE structure.[7] Among various high-*k* dielectrics, HfON (Refs. 3 and 4) and Y_2O_3 (Ref. 5) have been identified as promising CTL candidates due to their high P/E speeds and large memory window. Furthermore, both HfON and Y_2O_3 show some distinctive characteristics. For HfON, it has a high *k* value (~22), small conduction-band offset with respect to Si ($\Delta E_c = 1.5$ eV), and low interface-state density when contacting with SiO_2, all of which can improve the P/E speeds and retention property of the CTN memory.[8–10] The main problems of HfON lie in its large elemental diffusion coefficient.[8] On the contrary, Y_2O_3 can act as an effective blocking barrier to suppress element inter-diffusion.[11] The shortcomings of Y_2O_3 include its relatively low *k* value (~15), high ΔE_c (~2.3 eV), and poor interface with SiO_2.[8,10] So, it is obvious that the characteristics of HfON and Y_2O_3 are mutually complementary. In this work, based on metal-nitride-oxide-silicon (MNOS) and metal-alumina-nitride-oxide-silicon (MANOS) capacitors, the charge-trapping characteristics of HfYON are studied for CTN memory applications with a view that HfYON could inherit the advantages of both HfON and Y_2O_3. Experimental data show that the HfYON film can indeed have better charge-trapping characteristics than the HfON and Y_2O_3 films.

Both MNOS and MANOS capacitors were fabricated on p-type (100) substrate. After a standard Radio corporation of America (RCA) clean, 3-nm thermal SiO_2 was grown on the wafers. Then, 12-nm HfYON was deposited by reactive co-sputtering of Hf and Y targets in a mixed ambient (Ar/N_2 = 4:1). The samples were annealed in O_2 ambient at 500 °C for 15 s to transform HfYN to HfYON. After post-deposition annealing, Al was evaporated and patterned as gate electrodes followed by forming-gas annealing at 300 °C for 20 min. For comparison, MNOS capacitors with 12-nm HfON or Y_2O_3 were also fabricated using the same process, and denoted as HfON and Y_2O_3 samples, respectively. Besides, MANOS with 20-nm sputtered Al_2O_3 as blocking layer (Al/Al_2O_3/HfYON/SiO_2/Si) was also fabricated to check the availability of HfYON as the CTL for CTN memory applications. The thickness of the dielectrics was determined using ellipsometry and confirmed by transmission electron microscopy (TEM). The film composition and chemical bonding states were analyzed by x-ray photoelectron spectroscopy (XPS). The electrical characteristics were measured by HP4284A LCR meter and HP4156A semiconductor parameter analyzer.

The thickness of the HfYON/SiO_2 stack is 11.8 nm/3.1 nm from the cross-sectional TEM image shown in Fig. 1(a). Fig. 1(b) shows the Hf 4*f*, Y 3*d*, and O 1*s* XPS spectra of the HfYON sample. The composition of HfYON is determined to be $Hf_{0.05}Y_{0.23}O_{0.53}N_{0.19}$ by the XPS analysis. In Fig. 1(b), Hf 4*f* shows a doublet due to spin-orbit splitting into the Hf $4f_{5/2}$ and Hf $4f_{7/2}$ components at 19.3 and 17.8 eV, respectively. The two peaks fully agree with the values for HfON, indicating the presence of Hf–O–N bonding.[12] No evidence for Hf-silicate bonding (18.3 eV for Hf $4f_{7/2}$) is observed for the film.[13] Y 3*d* shows two strong peaks at 160.8 and 158.8 eV, corresponding to Y $3d_{3/2}$ and Y $3d_{5/2}$. The peak at 160.8 eV for Y $3d_{3/2}$ is higher than that at 156.8 eV for Y_2O_3.[14] These chemical shifts are in accordance with the formation of Y silicate (160.3 eV for Y $3d_{3/2}$ (Ref. 14)) and

a)Electronic mail: laip@eee.hku.hk.

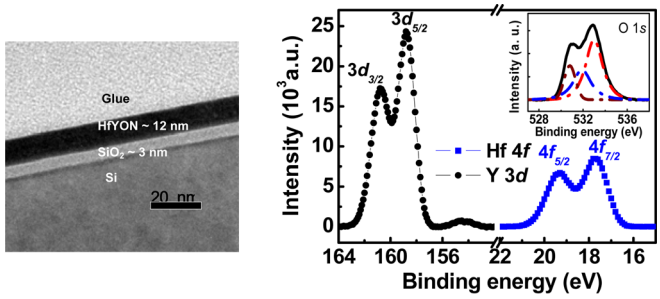

(a) (b)

FIG. 1. (Color online) (a) Cross-sectional TEM image of the MNOS sample with HfYON as CTL. (b) XPS spectrum of HfYON/SiO_2 stack (2 nm/3 nm) on Si substrate. The inset of (b) shows the O 1*s* spectrum (solid line) and its curve-fitting lines (dashed line).

the difference of the bonding energy (0.5 eV) should be due to nitrogen incorporation. The bonding structures can further be confirmed by the O 1*s* spectrum shown in the inset of Fig. 1(b), where the O 1*s* peak displays three components, corresponding to SiO_2 (533 eV) (Ref. 14), Y silicate (532 eV) (Ref. 14), and HfON (530.8 eV).

Fig. 2 depicts the 1 MHz C-V hysteresis loop of the MNOS capacitors under ±5-V sweeping voltage. All samples exhibit counterclockwise C-V loops, which are typical for memory devices. The initial flatband voltage (V_{FB}) is -1.1 ± 0.1 V for the samples. V_{FB} after forward sweeping is more positive (or more negative after backward sweeping) than the initial value, indicating that both electron-like and hole-like traps exist in the films. The Y_2O_3 sample has a larger V_{FB} shift of 2.0 V from the hysteresis C-V loop compared with 1.4 V of the HfON one, implying higher trap density in the Y_2O_3/SiO_2 stack. Among the devices, the largest hysteresis memory window (2.3 V) can be achieved for the HfYON sample, demonstrating its highest trapping efficiency. The HfYON film, consisting of Hf-related compound (HfON) and Y-related compound (Y silicate at the HfYON/SiO_2 interface) shown in Fig. 1(b), contributes to the excellent performance because both of them exhibit high trapping efficiency.[3–5]

To further confirm the difference in the charge-trapping characteristics of the MNOS capacitors, the charge-trap centroid measured from the metal/oxide interface (X_t, nm) and charge-trap density (N_t, cm^{-2}) are extracted by the constant-current stress (CCS) method[15]

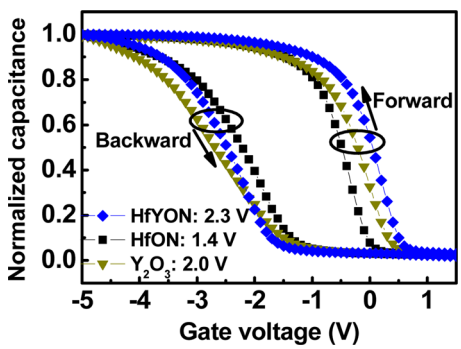

FIG. 2. (Color online) 1-MHz C-V hysterisis curves of the MNOS samples under ±5-V sweeping gate voltage. The hysterisis memory window for each sample is also shown in the figure.

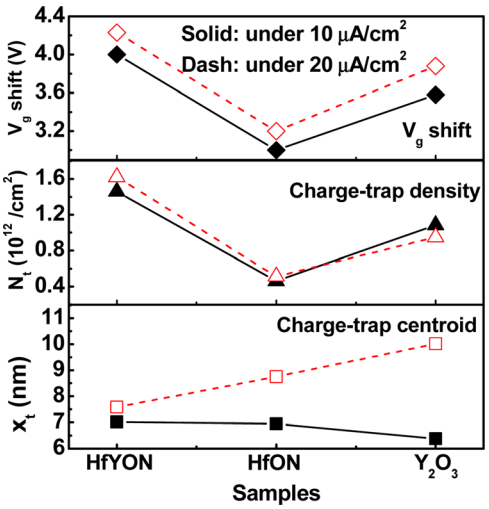

FIG. 3. (Color online) Charge-trap centroid (square symbol), charge-trap density (triangle symbol), and gate-voltage shift (diamond symbol) induced by a constant-current stress at positive 10-μA/cm^2 and 20-μA/cm^2.

$$X_t = t_{ox}\left(1 - \frac{\Delta V_{-g}}{\Delta V_{+g}}\right)^{-1}, \tag{1}$$

$$N_t = \frac{\varepsilon_0 \varepsilon_{ox}}{q t_{ox}}(\Delta V_{-g} - \Delta V_{+g}), \tag{2}$$

where t_{ox} and ε_{ox} are thickness and relative permittivity of the gate oxide; ΔV_{-g} and ΔV_{+g} are the negative and positive gate-voltage shifts. Fig. 3 summarizes the extracted values of X_t and N_t, as well as the measured gate voltage shift (ΔV_g) under positive 10-μA/cm^2 and 20-μA/cm^2 constant-current stresses (corresponding to electron injection from the Si substrate), respectively. ΔV_g is induced due to electron trapping in the dielectric stack. The HfYON sample shows larger ΔV_g and N_t, indicating its higher trapping efficiency. It is also observed that different from the HfON and HfYON samples, the N_t of the Y_2O_3 sample decreases with increasing the value of current stress, which should be ascribed to stress-induced leakage in the Y_2O_3 sample.[8] The X_t of the samples moves towards the SiO_2 side with increasing stress, implying that injected electrons tend to fill the traps near the gate side first, which is beneficial for the retention characteristics by avoiding electrons tunneling back to the substrate. The X_t shift of the Y_2O_3 sample under CCS is much closer to the SiO_2 side

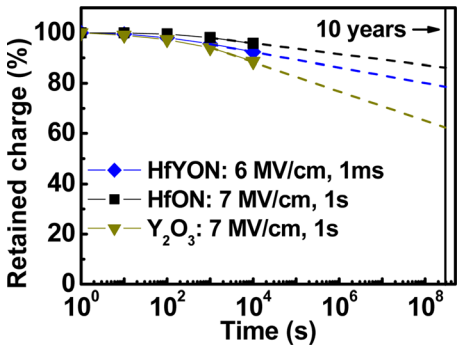

FIG. 4. (Color online) Retention characteristics of the MANOS samples at room temperature. All samples are programmed to achieve the same initial memory window for the measurement.

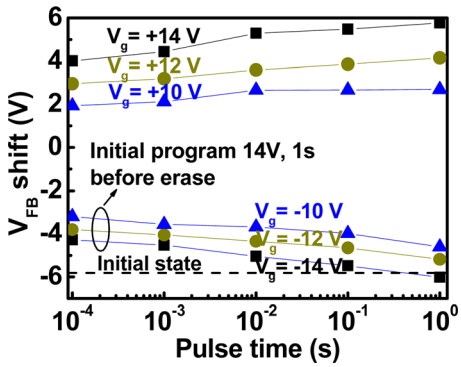

FIG. 5. (Color online) P/E characteristics of the MANOS sample with HfYON as CTL for various gate voltages.

than those of the HfYON and HfON ones. Consequently, interface traps are dominant for the Y_2O_3 film, whereas bulk traps are dominant for the HfYON and HfON films. Moreover, the smaller X_t shift (0.56 nm) for the HfYON sample demonstrates its higher trapping efficiency compared with the HfON (1.81 nm) and Y_2O_3 ones (3.64 nm).

Fig. 4 shows the retention characteristics of the MANOS capacitors measured at room temperature. All the samples are programmed with an initial memory window of ~2.1 V. For the HfYON sample, a lower gate voltage with shorter programming period (6 MV/cm, 1 ms) can be used to achieve the same memory window as the HfON (7 MV/cm, 1 s) and Y_2O_3 (7 MV/cm, 1 s) ones, mainly due to its higher trapping efficiency as mentioned above. The retained charge rate after 10 years is evaluated by extrapolation to be 79%, 86%, and 62% for the HfYON, HfON, and Y_2O_3 MANOS samples, respectively. It is noted that both of the HfYON and HfON samples display better retention characteristics than the Y_2O_3 one. This can be ascribed to more bulk traps and less interface traps in the HfYON and HfON films, because bulk traps should be more immune to tunneling of electrons back to the substrate than interface traps. Fig. 5 shows the P/E characteristics of the MANOS capacitor with HfYON as the CTL. The V_{FB} shift is 4.5 V after stressing at +14 V for 1 ms. A large memory window of 6.0 V is obtained by ±14 V for 1 s. Moreover, negligible over-erase phenomenon is observed under the erase state.

In summary, the charge-trapping characteristics of HfYON are investigated based on MNOS and MANOS capacitors. Compared with the samples with HfON or Y_2O_3 as CTL, the proposed MNOS sample shows better charge-trapping characteristics mainly due to higher trapping efficiency, which are confirmed by extracting their charge-trap centroid and charge-trap density by the CCS method. Moreover, the excellent performance of the proposed MANOS capacitor with HfYON as CTL further supports that HfYON is a promising candidate as the charge-trapping layer for high performance charge-trapping nonvolatile memory applications.

This work is financially supported by the University Development Fund (Nanotechnology Research Institute, 00600009) of the University of Hong Kong and the National Natural Science Foundation of China (Grant no. 60976091).

[1]X. G. Wang, J. Liu, W. P. Bai, and D. L. Kwong, IEEE Trans. Electron Devices **51**, 597 (2008).
[2]C. H. Chang and J. G. Hwu, J. Appl. Phys. **105**, 094103 (2009).
[3]H. J. Yang, C. F. Cheng, W. B. Chen, S. H. Lin, F. S. Yeh, S. P. McAlister, and A. Chin, IEEE Trans. Electron Devices **55**, 1417 (2008).
[4]J. Y. Wu, Y. T. Chen, M. H. Lin, and T. B. Wu, IEEE Electron Device Lett. **31**, 993 (2010).
[5]T. M. Pan and W. W. Yeh, IEEE Trans. Electron Devices **55**, 2354 (2008).
[6]Y. H. Wu, L. L. Chen, Y. S. Lin, M. Y. Li, and H. C. Wu, IEEE Electron Device Lett. **30**, 1290 (2009).
[7]S. H. Lin, A. Chin, F. S. Yeh, and S. P. McAlister, Tech. Dig. - Int. Electron Devices Meet. **2008**, 843 (2008).
[8]G. D. Wilk, R. M. Wallace, and J. M. Anthony, J. Appl. Phys. **89**, 5243 (2001).
[9]G. Shang, P. W. Peacock, and J. Robertson, Appl. Phys. Lett. **84**, 106 (2004).
[10]M. Copel, N. Bojarczuk, L. F. Edge, and S. Guha, Appl. Phys. Lett. **97**, 182901 (2010).
[11]C. X. Li and P. T. Lai, Appl. Phys. Lett. **95**, 022910 (2009).
[12]K. Y. Tong, E. V. Jelenkovic, W. Liu, and J. Y. Dai, Microelectron. Eng. **83**, 293 (2006).
[13]O. Renault, D. Samour, J. F. Damlencourt, D. Blin, F. Martin, and S. Marthon, Appl. Phys. Lett. **81**, 3627 (2002).
[14]J. J. Chambers and G. N. Parsons, J. Appl. Phys. **90**, 918 (2001).
[15]Z. H. Liu, P. T. Lai, and Y. C. Cheng, IEEE Trans. Electron Devices **38**, 344 (1991).